Advances in Analytical Chemistry 2015, 5(3A): 19-25
DOI: 10.5923/s.aac.201501.03

Inhibitory Effect of Newly Synthesized Organic Compound in Corrosion of Aluminum: Electrochemical Investigation

Ali Ehsani[1,2,*], Malihe Ahmadi[1], Mohammad Ghanbari[2]

[1]Department of Chemistry, Faculty of science, University of Qom, Qom, Iran
[2]Department of Chemistry, Payame Noor University, Iran

Abstract New synthesized 1-(4-nitrophenyl)-5-amino-1*H*-tetrazole s inhibitory effect on the corrosion of aluminium (Al) in sulfuric acid was investigated by means of potentiodynamic polarization and electrochemical impedance spectroscopy (EIS). According to electrochemical results, excellent inhibiting properties for SS corrosion in sulfuric acid has been obtained. The adsorption of 1-(4-nitrophenyl)-5-amino-1*H*-tetrazole onto the Al surface followed the Langmuir adsorption model with the free energy of adsorption ΔG^0_{ads} of -11.25 kJ mol^{-1}. Quantum chemical calculations were employed to give further insight into the mechanism of inhibition action of 1-(4-nitrophenyl)-5-amino-1*H*-tetrazole.

Keywords Organic inhibitor, Adsorption, Aluminum, Impedance, Nanoparticles

1. Introduction

Aluminium and aluminium alloys represent an important category of materials due to their high technological value and wide range of industrial applications, especially in aerospace and household industries [1]. Owing to these applications of aluminium and its alloys, considerable attention has been devoted to the corrosion behaviour of these materials in various aggressive environments [2–6]. It is well known that aluminium is usually protected by a thin oxide film which has been formed either spontaneously (native film) or deliberately (e.g. anodic films). The solubility of the oxide film is negligible in neutral solutions (pH interval 4.0–8.5) at room temperature, whereas heavy corrosion is observed both in highly acidic and alkaline media [2, 7]. Acidic solutions are used for pickling, chemical and electrochemical etching of aluminium.

Therefore, inhibition of aluminium corrosion in acidic media has a great importance [8, 9].

The use of organic molecules containing functional groups and p electrons in their structure as corrosion inhibitor is one of the most practical methods for protecting metals against the corrosion and it is becoming increasingly popular. The existing data show that organic inhibitors act by the adsorption and protect the metal by film formation. Organic compounds bearing heteroatoms with high electron density such as phosphor, sulphur, nitrogen, oxygen or those containing multiple bonds which are considered as adsorption centers, are effective as corrosion inhibitor [10–14]. The compounds contain both nitrogen and sulphur in their molecular structure have exhibited greater inhibition compared with those contain only one of these atoms [15–17]. In literature many thiazole derivatives have been studied as corrosion inhibitor and found that thiazole derivatives have good corrosion inhibition effect [18, 19]. The efficiency of an organic compound inhibitor is mainly dependent on its ability to adsorb on a metal surface which consists of replacement of a water molecule at a corroding interface. In this study electrochemical tests were employed to investigate the inhibition performance of new synthesized 1-(4-nitrophenyl)-5-amino-1*H*-tetrazole inhibitor in acidic solution.

* Corresponding author:
ehsani46847@yahoo.com (Ali Ehsani)
Published online at http://journal.sapub.org/aac

2. Experimental

2.1. Materials and Apparatus

Aluminum having composition (wt %) Al 99.8, Ni 0. 01, Si 0.1, Mn 0.006, Mg 0.005, Cu 0.01, Pb 0.03, Bi 0.005, Co 0.002, Ti 0.002, Na 0.001, Fe 0.05, Ga 0.005. The exposed surface of working electrode (Al) was ground with silicon carbide abrasive paper from 400 to 1200, degreased with absolute ethanol, rinsed in distilled water, and dried in warm air. The corrosive medium was 0.5 M H_2SO_4 solution prepared from analytical-reagent-grade 98% sulfuric acid and distilled water. Synthesis of 1-(4-nitrophenyl)-5-amino-1*H*-tetrazole nanoparticles was

prepared according to the literature [20]. A mixture of the 4-nitrophenylcyanamide (2 mmol), NaN_3 (3 mmol), and $ZnCl_2$ (2 mmol) in H_2O (16 mL) was ultrasonicated for 15 h at 70-80 ℃. The reaction mixture was cooled to 25 ℃, the solid residue was filtered, washed with H_2O and treated with 3 M HCl (4 mL). The crude product was purified by aqueous ethanol to afford the pure product. The concentration range of 1-(4-nitrophenyl)-5-amino-1H-tetrazole) employed was 1×10^{-4} to 10^{-3} M in 0.5 M sulfuric acid. SEM micrograph of synthesized 1-(4-nitrophenyl)-5-amino-1H-tetrazole is presented in Fig. 1.

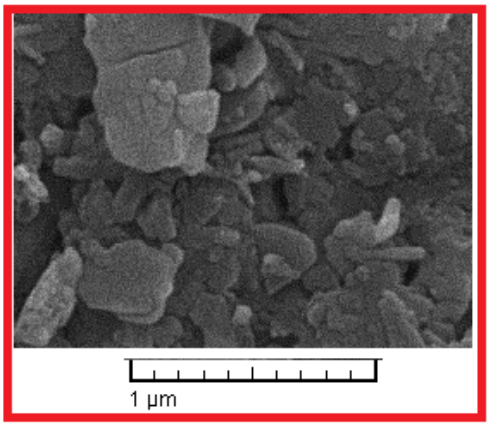

Figure 1. SEM micrograph of synthesized 1-(4-nitrophenyl)-5-amino-1H-tetrazole

The concentration range of 1-(4-nitrophenyl)-5-amino-1*H*-tetrazole employed was 1×10^{-4} to 10^{-3} M in 0.5 M sulfuric acid. All electrochemical experiments were carried out by an Autolab General Purpose System PGSTAT 30 (Eco-chime, Netherlands). The frequency range of 100 kHz to 15 mHz and modulation amplitude of 5 mV were employed for impedance studies. A saturated calomel electrode (SCE) and a platinum wire were used as reference and counter electrodes respectively. Before measurement, the working electrode was immersed in test solution for approximately 1 h until a steady open-circuit potential (OCP) was reached. The polarization curves were carried out from cathodic potential of -1.4 V to anodic potential of 0.10 V with respect to the open circuit potential at a sweep rate of 0.5 mV/s. The linear Tafel segments of the anodic and cathodic curves were extrapolated to corrosion potential (E_{corr}) to obtain the corrosion current (i_{corr}). In each measurement, a fresh working electrode was used. Several runs were performed for each measurement to obtain reproducible data.

3. Results and Discussion

3.1. Potentiodynamic Polarization Studies

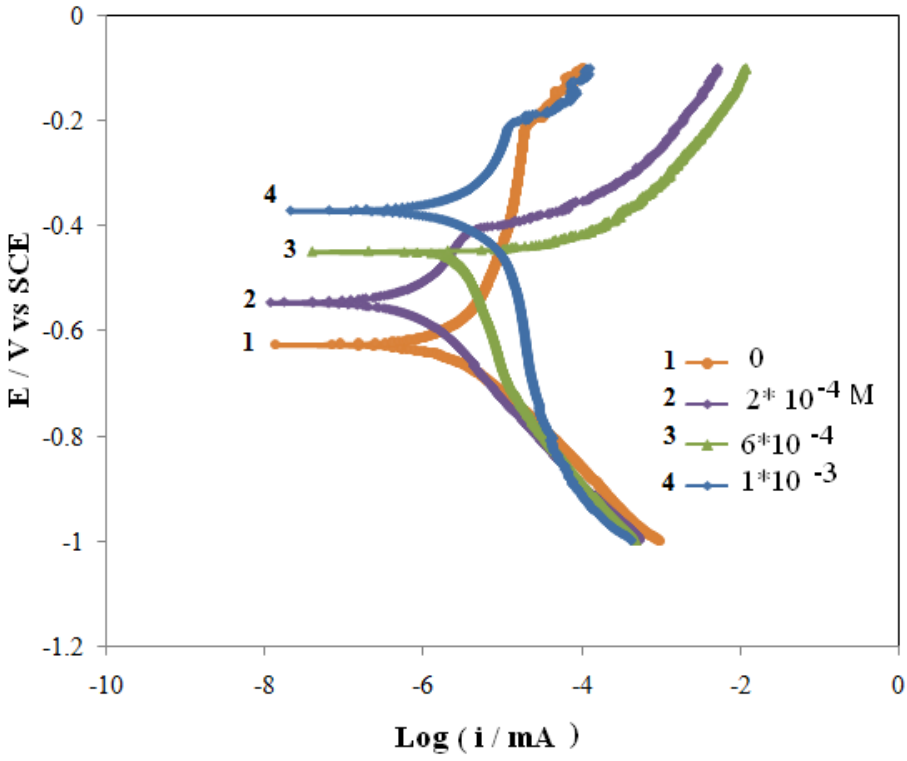

Figure 2. Potentiodynamic polarisation curves of aluminium in 0.5 M H_2SO_4 solution in the absence and presence of various concentrations of the 1-(4-nitrophenyl)-5-amino-1*H*-tetrazole

Table 1. Corrosion parameters obtained from Tafel polarisation curves of aluminium in 0.5M H_2SO_4 in the absence and presence of different concentrations of 1-(4-nitrophenyl)-5-amino-1*H*-tetrazole at 298 K

[Inhibitor]	Inhi. Con.	Ba(v/decade)	Bc(v/dedade)	I (uA)	E(v)	CR(mpy)
0	0	0.45	0.15	2.1	-0.66	0.9
0.0001	0.001	0.43	0.17	2.01	-0.63	0.82
0.0002	0.002	0.40	0.17	1.94	-0.61	0.76
0.0004	0.004	0.32	0.15	1.67	-0.54	0.71
0.0006	0.006	0.33	0.22	1.56	-0.44	0.66
0.0008	0.008	0.10	0.23	1.34	-0.43	0.57
0.001	0.01	0.09	0.2	0.86	-0.37	0.36

Polarization measurements were carried out to get information regarding the kinetics of anodic and cathodic reactions. The potentiodynamic polarization curves for Al in 0.5 M H_2SO_4 Solution in the absence and presence of different concentrations of the inhibitor molecules are shown in Fig.2. The values of electrochemical kinetic parameters such as corrosion potential (E_{corr}), corrosion current (i_{corr}) and Tafel slopes, determined from these by extrapolation method, are listed in Table 1. In corrosion, quantitative information on corrosion currents and corrosion potentials can be extracted from the slope of the curves, using the Stern-Geary equation, as follows [21]:

$$i_{corr} = \frac{1}{2.303R_p}\left(\frac{\beta_a \times \beta_c}{\beta_a + \beta_c}\right) \quad (1)$$

i_{corr} is the corrosion current in Amps; R_p is the corrosion resistance in ohms;

β_a is the anodic Tafel slope in Volts/decade or mV/decade of current density; β_c is the cathodic Tafel slope in Volts/decade or mV/decade of current density; the quantity, $\frac{\beta_a \times \beta_c}{\beta_a + \beta_c}$, is referred to as the Tafel constant. The corrosion inhibition efficiency was calculated using the relation:

$$\eta(\%) = 100\left(\frac{i^*_{corr} - i_{corr}}{i^*_{corr}}\right) \quad (2)$$

where i_{corr}* and i_{corr} are uninhibited and inhibited corrosion current, respectively, determined by extrapolation of Tafel lines in the corrosion potential. The corrosion rates ν (mm $year^{-1}$) from polarization were calculated using the following Equation:

$$\upsilon = \frac{i_{corr} \times t \times M}{F \times S \times d} \times 10$$

where t is the time (s), M is the equivalent molar weight of Al (g mol^{-1}), F is Faraday constant (96500 $Cmol^{-1}$), S is the surface area of electrode, d is the density of iron, the constant 10 is used to convert the unit cm to mm. The results are presented in table 1. The inhibitor molecule first adsorbs on the Al surface and blocks the available reaction sites. As concentration of the inhibitor increases the linear polarization resistance increases and corrosion rate (CR) decreases. The surface coverage increases with the inhibitor concentration and the formation of inhibitor film on the Al surface reduces the active surface area available for the attack of the corrosive medium and delays hydrogen evolution and metal dissolution [22]. In cathodic domain, as seen in Table 1, the values of βc had small changes with increasing inhibitor concentration, which indicated that the 1-(4-nitrophenyl)-5-amino-1*H*-tetrazole was adsorbed on the metal surface and the addition of the inhibitor hindered the acid attack on the Al electrode. In anodic domain, the value of βa decreases with the presence of 1-(4-nitrophenyl)-5-amino-1*H*-tetrazole. The shift in the anodic Tafel slope βa might be attributed to the modification of anodic dissolution process due to the inhibitor modules adsorption on the active sites. Compared to the absence of 1-(4-nitrophenyl)-5-amino-1*H*-tetrazole, the anodic curves of the working electrode in the acidic solution containing the 1-(4-nitrophenyl)-5-amino-1*H*-tetrazole shifted obviously to the direction of current reduction, as it could be seen from these polarization results; the inhibition efficiency increased with inhibitor concentration.

3.2. Electrochemical Impedance Spectroscopy

Electrochemical impedance spectroscopy is one of the best techniques for analyzing the properties of conducting polymer electrodes and charge transfer mechanism in the electrolyte/electrode interface. It has been broadly discussed in the literature using a variety of theoretical models [23-27]. Impedance measurements were performed under potentiostatic conditions after 1 h of immersion. Nyquist plots of uninhibited and inhibited solutions containing different concentrations of inhibitor molecules were performed over the frequency range from 100 kHz to 100 mHz and are shown in Fig. 3. The Nyquist diagrams show one capacitive loop at high frequencies. The capacitive loop at high frequencies represents the phenomenon associated with the electrical double layer. The above impedance diagrams (Nyquist) contain depressed semicircles with the centre under the real axis. Such behavior is characteristic of solid electrodes and often referred to frequency dispersion, attributed to different physical phenomena such as roughness, inhomogeneities of the solid surfaces, impurities, grain boundaries, and distribution of surface active sites. The ideal capacitive behavior is not seen in this case and hence a

constant phase element CPE is introduced in the circuit to give a more accurate fit [23-27]. The mechanism of corrosion remains unaffected during the addition of inhibitor molecules. The simplest fitting is represented by Randle's equivalent circuit (Fig. 3), which is a parallel combination of the charge-transfer resistance (R_{ct}) and the constant phase element (CPE), both in series with the solution resistance (R_s). The impedance function of a CPE can be represented as:

$$Z_{CPE} = Y_0^{-1}(j\omega)^{-n} \quad (3)$$

where Y_0 is the CPE constant, ω is the angular frequency, and n is the CPE exponent which can be used as a gauge of the heterogeneity or roughness of the surface[26, 27]. In the present work, the value of n has a tendency to decrease with increasing inhibitor concentration, which may be attributed to the increase of inhibitor concentration resulted in the increasing surface roughness. For a circuit including a CPE, the C_{dl} could be calculated from CPE parameter values Y_0 and n using the expression [26]:

$$C_{dl} = Y_0(\omega''_m)^{-n} \quad (4)$$

where C_{dl} is the double layer capacitance and ω''_m is the frequency at which the imaginary part of the impedance has a maximum. As seen from Table 2, the double layer capacitance (C_{dl}) decreases with increase in concentration. This can be attributed to the gradual replacement of water molecules by the adsorption of the organic molecules at metal/solution interface, which is leading to a protective film on metal surface. In addition, the more the inhibitor is adsorbed, the more the thickness of the barrier layer is increased according to the expression of the Helmholtz model [28]:

$$C_{dl} = \frac{\varepsilon\varepsilon_0 A}{d} \quad (5)$$

where d is the thickness of the protective layer, e is the dielectric constant of the medium, ε_0 is the vacuum permittivity and A is the surface area of the electrode. The equation used for calculating the percentage inhibition efficiency is:

$$\eta(\%) = 100\left(\frac{Rp^* - Rp}{Rp^*}\right) \quad (6)$$

where R_p* and R_p are values of the polarisation resistance observed in the presence and absence of inhibitor molecules. Impedance parameters are summarized in Table 2. The presence of the inductive might be attributed to the relaxation process obtained by adsorption species as H_{ads} and SO_4^{2-} on the electrode surface. Similar findings were reported in already published papers [29-31] during the corrosion behavior of pure Al in acidic solutions containing chloride ion. As seen in Table 2, which present impedance parameters compatible with presented equivalent circuit [22], the adsorption of 1-(4-nitrophenyl)-5-amino-1*H*-tetrazole molecules on Al surface modifies the interface between the corrosive medium and metal surface and decreases its electrical capacity. The increase in R_{ct} values with increase in 1-(4-nitrophenyl)-5-amino-1*H*-tetrazole concentration could be interpreted as formation of an insulated adsorption layer. At the highest inhibitor concentration of 10^{-3} mol/L, the inhibition efficiency was increased.

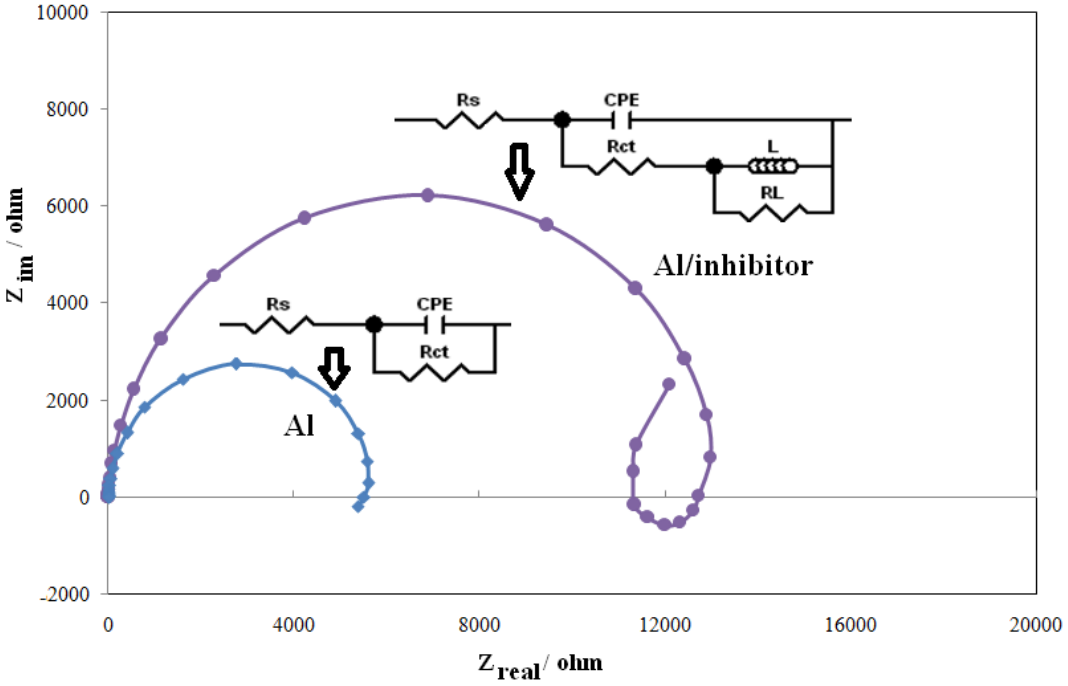

Figure 3. Nyquist plots of aluminium in 0.5 M H_2SO_4 solution in the absence and presence of 1-(4-nitrophenyl)-5-amino-1*H*-tetrazole. Electrical equivalent circuit used for modeling metal/solution interface in the absence and presence of inhibitors

Table 2. Impedance parameters for the corrosion of Al in 0.5M H_2SO_4 containing different concentration of 1-(4-nitrophenyl)-5-amino-1*H*-tetrazole at 298 K

Concentration x (M)	R_s (Ω)	Y_0 ($\mu\ \Omega^{-1}\ S^n$)	n	R_{ct} (Ω)	R_L (Ω)	L (H)	C_{dl} (μ F)
0	1.58	85.14	0.93	5712			110.25
2.0×10^{-4}	1.85	65.18	0.89	7528	542	20.17	98.57
4.0×10^{-4}	2.14	58.14	0.87	8562	675	59.82	86.35
6.0×10^{-4}	2.85	45.13	0. 87	9852	852	120.38	69.28
8.0×10^{-4}	3.25	38.19	0. 83	10468	1268	220.61	48.14
1.0×10^{-3}	3.87	36.14	0.79	12158	1515	300.45	43.78

3.3. Adsorption Isotherms

The adsorption of an organic adsorbate at metal/solution interface can be presented as a substitution adsorption process between the organic molecules in aqueous solution, (Org_{aq}), and the water molecules on metallic surface, (H_2O_{ads}) Org_{aq}

$$Org_{aq} + nH_2O_{ads} \leftrightarrow Org_{ads} + nH_2O_{aq} \quad (9)$$

where n, the size ratio, is the number of water molecules displaced by one molecule of organic inhibitor. X is assumed to be independent of coverage or charge on the electrode [30]. Basic information on the interaction between the inhibitors and the steel surface is provided by the adsorption isotherm. The degree of surface coverage, θ, at different inhibitor concentrations in 0.5 M H_2SO_4 was evaluated from impedance measurment (θ = IE(%)/100) at 25 ℃. The plot of C/θ against inhibitor oncentration C displayed a straight line for tested inhibitor (Fig. 4). The linear plot clearly revealed that the surface adsorption process of 1-(4-nitrophenyl)-5-amino-1*H*-tetrazole on the Al surface obeys the Langmuir isotherm. Likewise, it suggests that an adsorption process occurs, which can be expressed as follows [30]:

$$\frac{C}{\theta} = \frac{1}{K_{ads}} + C \quad (10)$$

where K_{ads} is the equilibrium constant of the adsorption process. Free energy of adsorption (ΔG_{ads}) can be calculated by Eq. (11). The numeral of 55.5 is the molar concentration of water in the solution:

$$K_{ads} = \frac{1}{55.5}\exp\left(\frac{-\Delta G^0_{ads}}{RT}\right) \quad (11)$$

The value of ΔG^0 ads for adsorption of 1-(4-nitrophenyl)-5-amino-1*H*-tetrazole was found to be -11.25kJ mol^{-1}. The negative value of ΔG^0 ads suggests that 1-(4-nitrophenyl)-5-amino-1*H*-tetrazole is spontaneously adsorbed on the Al surface. Literature survey reveals that the values of ΔG^0 ads around -20 kJ mol^{-1} or lower are consistent with the electrostatic interaction between the charged molecules and the charged metal (physical adsorption) [32]. The adsorption of an inhibitor on the metal surface can occur on the basis of donor–acceptor interactions between the p-electrons of the heterocyclic compound and the vacant d-orbitals of the metal surface atoms, so the energies of the frontier orbital's should be considered. Energy of LUMO depicts the ability of the molecule to receive charge when attacked by electron pair donors, even as the energy of HOMO to donate the charge when attached by electron seeking reagents. As the energy gap between the frontiers orbital's get smaller, the interactions between the reacting species get stronger [33]. In this regards, the electronic properties such as highest occupied molecular orbital (HOMO) energy, lowest unoccupied molecular orbital (LUMO) energy and frontier molecular orbital coefficients have been calculated for prepared inhibitor. The natural bond orbital (NBO) analysis was applied to determine the atomic charges. Results are presented in Figure 5. According to the results, HOMO location in the 1-(4-nitrophenyl)-5-amino-1*H*-tetrazole molecule is mostly distributed in the vicinity of the nitrogen, oxygen atoms and the aromatic rings of the benzoquinoxaline moiety. This indicates the reactive sites of the interaction between 1-(4-nitrophenyl)-5-amino-1*H*-tetrazole and the Al surface. Mulliken population analysis has been presented in Fig. 5e is further evidence for interaction between Al surface and inhibitor active sites. It is clear from the figure 4 that the nitrogen atoms of 1-(4-nitrophenyl)-5-amino-1*H*-tetrazole have considerable excess of negative charge than other atoms. Thus, the adsorption of 1-(4-nitrophenyl)-5-amino-1*H*-tetrazole as neutral molecules on the metal surface can occur directly involving the displacement of water molecules from the metal surface and sharing of electrons between the nitrogen atoms and the metal surface. It should be noted that 1-(4-nitrophenyl)-5-amino-1*H*-tetrazole adsorb mainly through electrostatic interactions between the positively charged nitrogen atom (since acidic solution can protonate the nitrogen atoms of 1-(4-nitrophenyl)-5-amino-1*H*-tetraz ole and the negatively charged metal surface (physisorption) as evident in the value of ΔG^0_{ads} obtained.

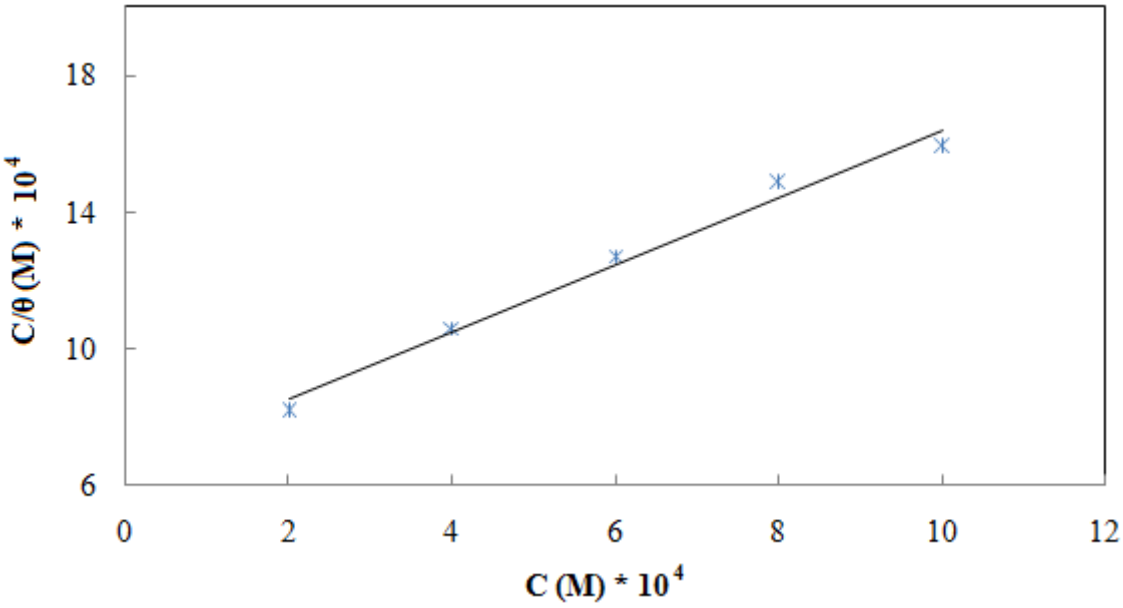

Figure 4. Langmuir adsorption plot for aluminium in 0.5 M H_2SO_4 containing different concentrations of 1-(4-nitrophenyl)-5-amino-1*H*-tetrazole

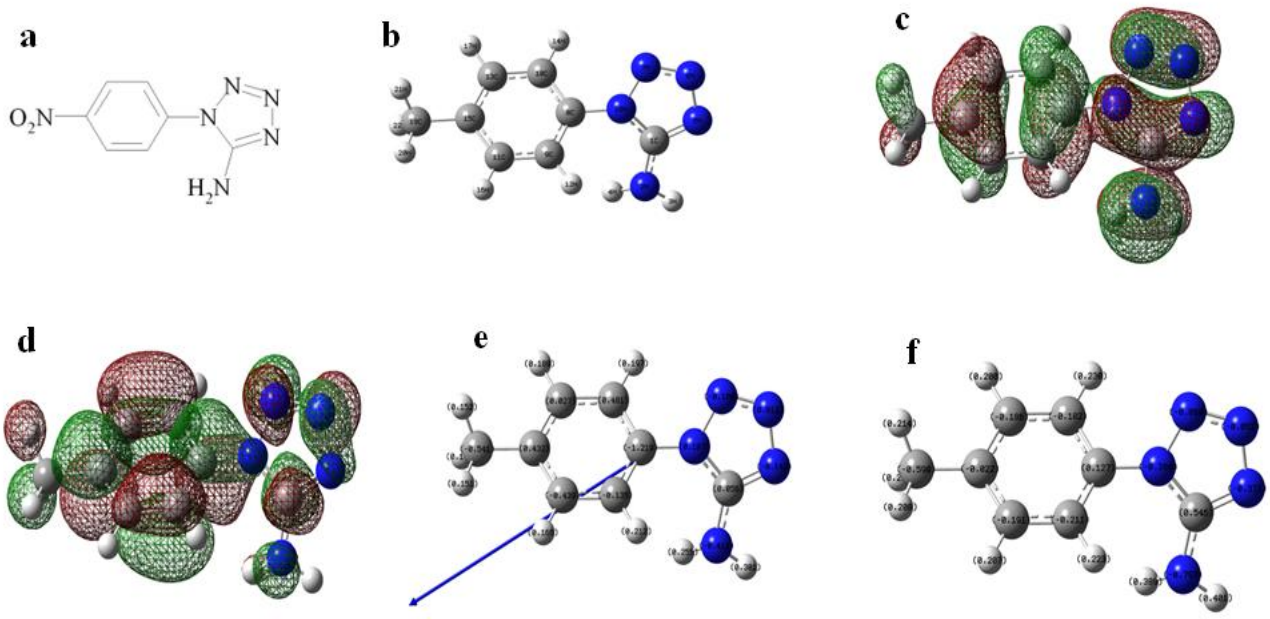

Figure 5. (a) Structure of 1-(4-nitrophenyl)-5-amino-1*H*-tetrazole; (b) Optimized molecular structure of 1-(4-nitrophenyl)-5-amino-1*H*-tetrazole, H atoms have been omitted for clarity; (c) The highest occupied molecular orbital (HOMO) of 1-(4-nitrophenyl)-5-amino-1*H*-tetrazole; (d) The lowest unoccupied molecular orbital (LUMO) of 1-(4-nitrophenyl)-5-amino-1*H*-tetrazole; (e) Muliken charge population analysis and vector of dipole moment of 1-(4-nitrophenyl)-5-amino-1*H*-tetrazole; (f) Natural charge population analysis of 1-(4-nitrophenyl)-5-amino-1*H*-tetrazole

4. Conclusions

1-(4-nitrophenyl)-5-amino-1*H*-tetrazole was found to inhibit the corrosion of Al in 0.5 M H_2SO_4 solution and the extent of inhibition was concentration dependent. Inhibition efficiency increases with increasing inhibitor concentration. EIS plots indicated that the charge transfer resistances increase with increasing concentration of the inhibitor; at the highest inhibitor concentration of 10^{-3} mol/L, the inhibition efficiency is increased. The 1-(4-nitrophenyl)-5-amino-1*H*-tetrazole inhibits the corrosion by getting adsorbed on the metal surface following Langmuir adsorption isotherm. Quantum chemical calculations show that the adsorption sites are mainly located around the nitrogen atoms of 1-(4-nitrophenyl)-5-amino-1*H*-tetrazole.

REFERENCES

[1] A.S. Fouda, A.A. Al-Sarawy, F.S. Ahmed, H.M. El-Abbasy, Corros. Sci. 51 (2009) 485–492.

[2] D. Mercier, M.G. Barthes-Labrousse, Corros. Sci. 51 (2009) 339–348.

[3] A.K. Maayta, N.A.F. Al-Rawashdeh, Corros. Sci. 46 (2004) 1129–1140.

[4] C.M.A. Brett, Corros. Sci. 33 (1992) 203–210.

[5] R. Grilli, M.A. Baker, J.E. Castle, B. Dunn, J.F. Watts, Corros. Sci. 52 (2010) 2855–2866.

[6] V. Moutarlier, M.P. Gigandet, B. Normand, J. Pagetti, Corros. Sci. 47 (2005) 937–951.

[7] M. Pourbaix, Atlas of Electrochemical Equilibria in Aqueous Solutions, Pergamon Press, London, 1966.

[8] H. Ashassi-Sorkhabi, B. Shabani, B. Aligholipour, D. Seifzadeh, Appl. Surf. Sci. 252 (2006) 4039–4047.

[9] M. Abdallah, Corros. Sci. 46 (2004) 1981–1996.

[10] J. Aljourani, K. Raeissi, M.A. Golozar, Corros. Sci. 51 (2009) 1836–1843.

[11] M.L. Zheludkevich, K.A. Yasakau, S.K. Poznyak, M.G.S. Ferreira, Corros. Sci. 47 (2005) 3368–3383.

[12] I.B. Obot, N.O. Obi-Egbedi, S.A. Umoren, Corros. Sci. 51 (2009) 276–282.

[13] M.G. Hosseini, M. Ehteshamzadeh, T. Shahrabi, Electrochim. Acta 52 (2007) 3680–3685.

[14] S, S_afak, B, Duran, A. Yurt, G. Turkoglu, Corrosion Science 54 (2012) 251–259.

[15] H.H. Hassan, E. Adbelghani, M.A. Amin, Electrochim. Acta 52 (2007) 6359–6366.

[16] Y. Abdoud, A. Abourrriche, T. Saffaj, M. Berrada, M. Charrouf, A. Bennamara, N. Al Himidi, H. Hannache, Mater. Chem. Phys. 105 (2007) 1–5.

[17] M.A. Quaraishi, J. Rawat, M. Ajmal, J. Appl. Electrochem. 30 (2000) 745– 751.

[18] K.F. Khaled, M.A. Amin, Corros. Sci. 51 (2009) 1964–1975.

[19] I.B. Obot, N.O. Obi-Egbedi, Corrosion Science 52 (2010) 282–285.

[20] D. Habibi, M. Nasrollahzadeh, H. Sahebekhtiari, R.V. Parish, Tetrahedron, 69 (2013), 3082-3087.

[21] M.G. Mahjani, R. Moshrefi, A. Ehsani, M. Jafarian, Anti corrosion method and material, 58 (2011) 250-257.

[22] T. Zhihua, Z. Shengtao, L. Weihua, H. Baorong , Ind. Eng. Chem. Res 50 (2011) 6082–6088.

[23] A. Ehsani, M.G. Mahjani, M. Jafarian, Turkish. Journal of chemistry, 35 (2011) 1-9.

[24] A. Ehsani, M. Nasrollahzadeh, MG. Mahjani, R. Moshrefi, H. Mostaanzadeh, Ind. Eng. Chem. 20(2014) 4363.

[25] A. Ehsani, M. G. Mahjani, M. Jafarian, A. Naeemy, Electrochim. Acta 71 (2012) 128-133.

[26] A. Ehsani, M.G. Mahjani, M. Jafarian, A. Naeemy, Prog. Org. Coat, 69 (2010) 510-516.

[27] A. Ehsani, MG. Mahjani, R. Moshrefi, H. Mostaanzadeh, J. Shabani Shayeh, *RSC. Adv. 4(2014)* 2231.

[28] Hassan, H. Electrochim. Acta 2006, 51, 5966–5972.

[29] H.J.W. Lenderink, M.V.D. Linden, J.H.W. DE Wit, Electrochim. Acta 38 (1993) 1989.

[30] Li. Xianghong, D. Shuduan, F. Hui, Corrosion Science 53 (2011) 1529-1536.

[31] K.F. Khaled, M.M. Al-Qahtani, Mater. Chem. Phys. 113 (2009) 150-158.

[32] S. Martinez, Mater. Chem. Phys. 2002, 77, 97–102.

[33] P. Hohenberg, W. Kohn, Phys. Rev. A136 (1964) 864.